



# Mantle viscosity derived from geoid and different land uplift data in Greenland

**Mohammad Bagherbandi<sup>1,2</sup>** , Hadi Amin<sup>1</sup> , Linsong Wang<sup>3,4</sup> and Masoud Shirazian<sup>5</sup>

1: Department of Computer and Spatial Sciences, University of Gävle, SE-80176 Gävle, Sweden

2: Division of Geodesy and Satellite Positioning, Royal Institute of Technology (KTH), SE-10044 Stockholm, Sweden

3: Hubei Subsurface Multi-scale Imaging Key Laboratory, Institute of Geophysics and Geomatics, China University of Geosciences, Wuhan, China.

4: Helmholtz Centre Potsdam, GFZ German Research Centre for Geosciences, Telegrafenberg, Potsdam, Germany.

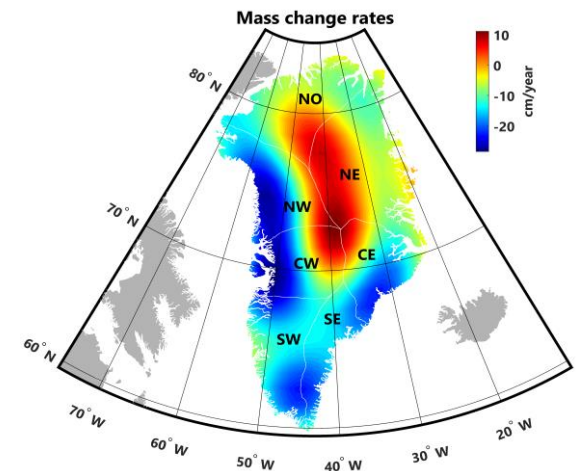
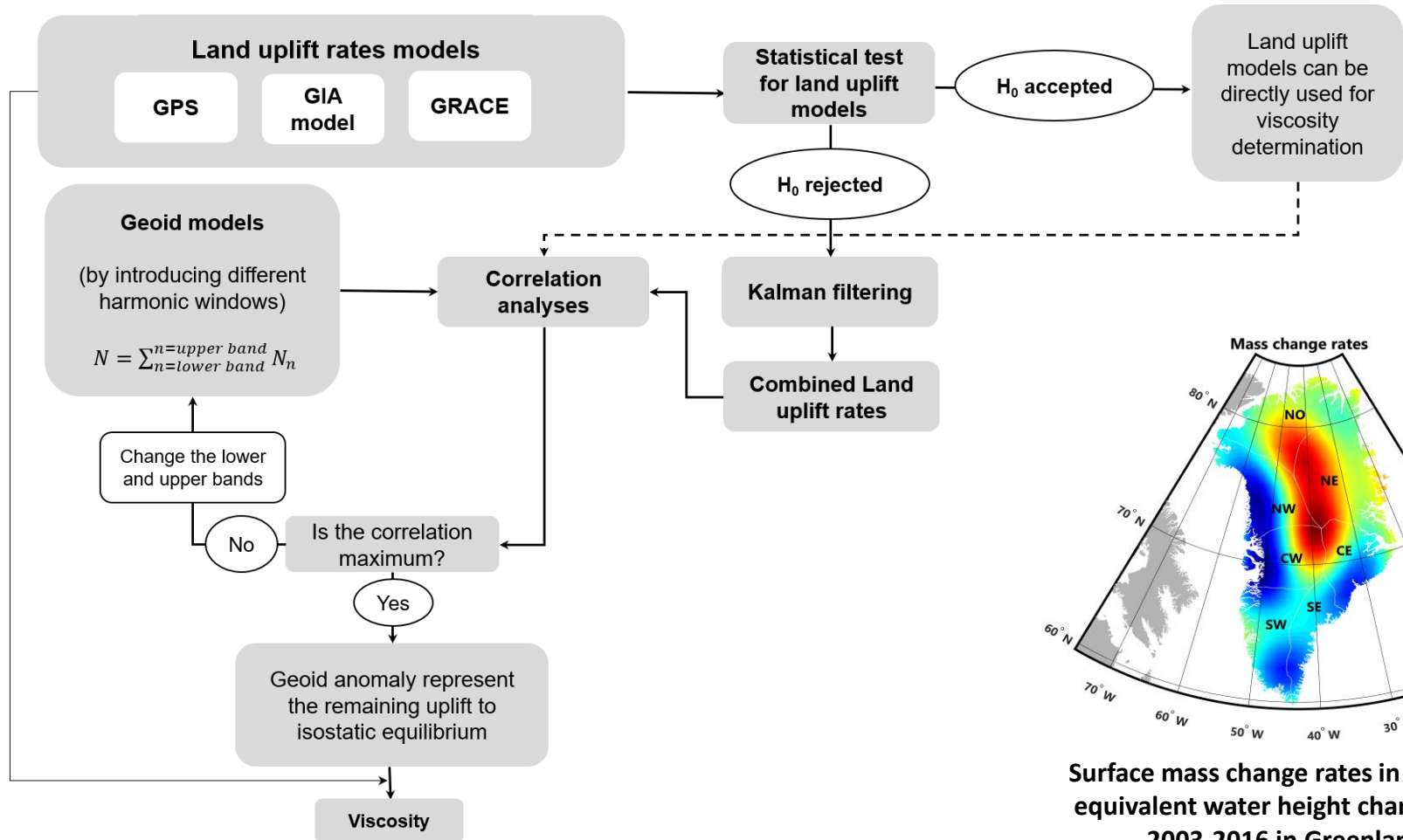
5: Department of geomatics engineering, Civil Engineering Faculty, Rajaee Teacher Training University, Tehran, Iran.



# Background and aim

- The Earth's mass redistribution due to deglaciation and recent ice sheet melting causes changes in the Earth's gravity field and vertical land motion.
- The changes are because of ongoing mass redistribution and related
  - elastic response (on a short time scale)
  - viscoelastic response (on time scales of a few thousands of years).
- **Aim:**
  - to infer the mantle viscosity associated with the glacial isostatic adjustment (GIA) and long-wavelength geoid beneath the Greenland lithosphere

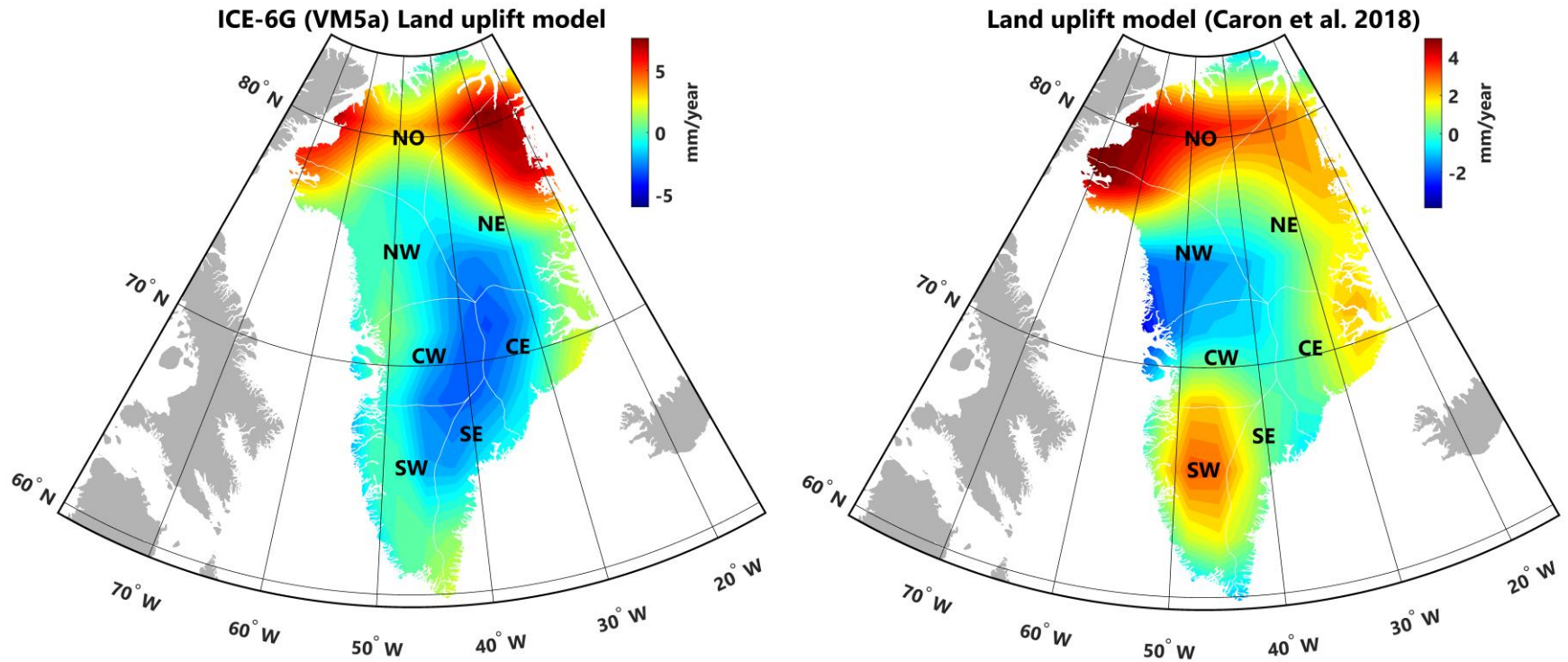
# Flowchart of viscosity determination using geoid anomaly and different land uplift rates



Surface mass change rates in terms of equivalent water height change over 2003-2016 in Greenland

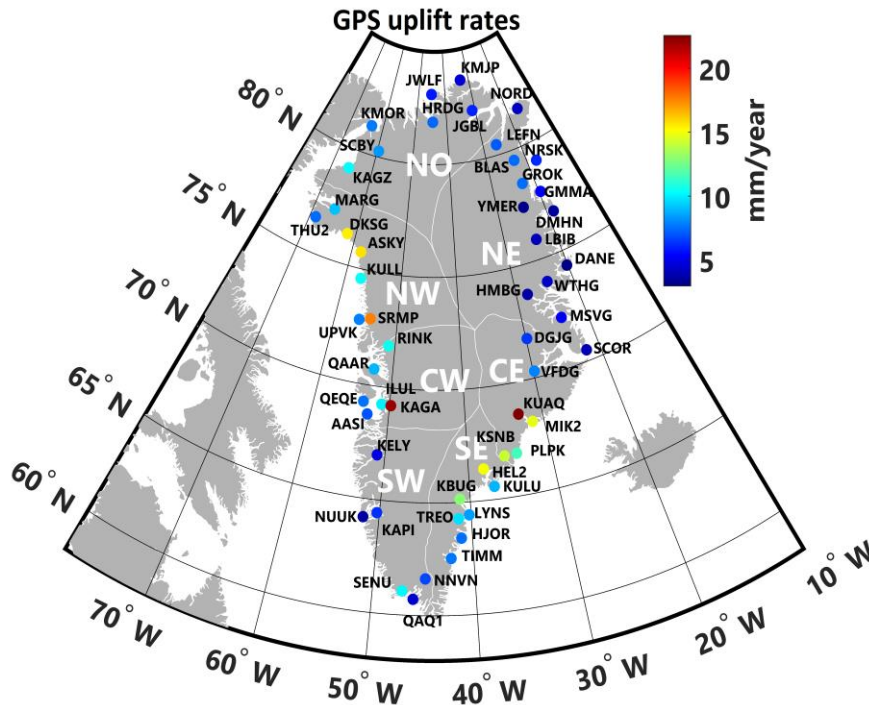
$$\eta \approx -\frac{\gamma^2}{4\pi G} \sum_{n=0}^{\infty} \frac{2n+1}{2n+4+3/n} \frac{N_n}{\dot{h}_n} \quad (\text{Sjöberg and Bagherbandi 2013})$$

# Land uplift rate: GIA models

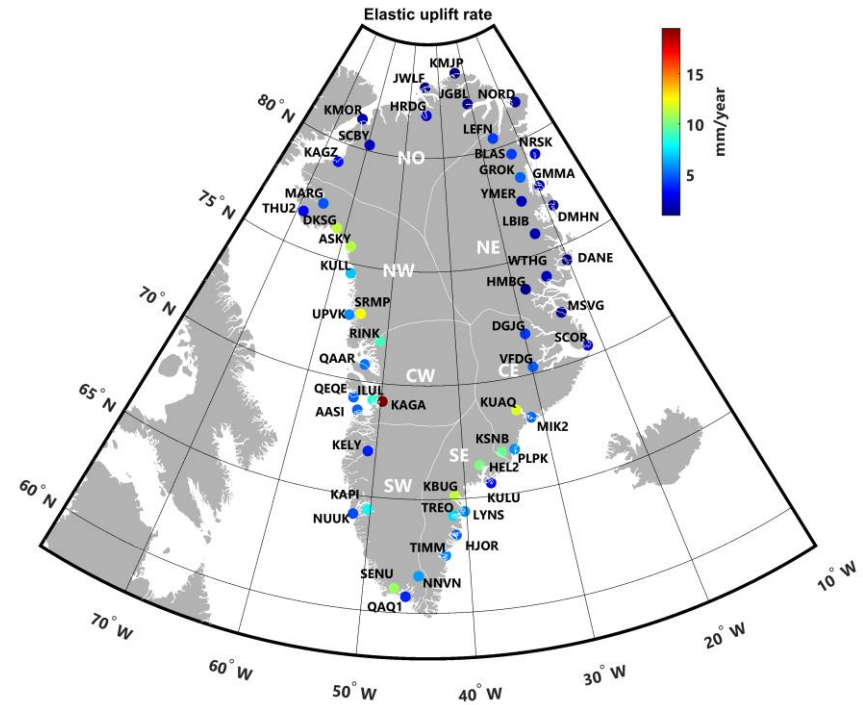


# Land uplift rate using GPS data

## 53 GNET GPS sites



Greenland Global Positioning  
System (GPS) Network (GNET)  
Khan et al. (2016)



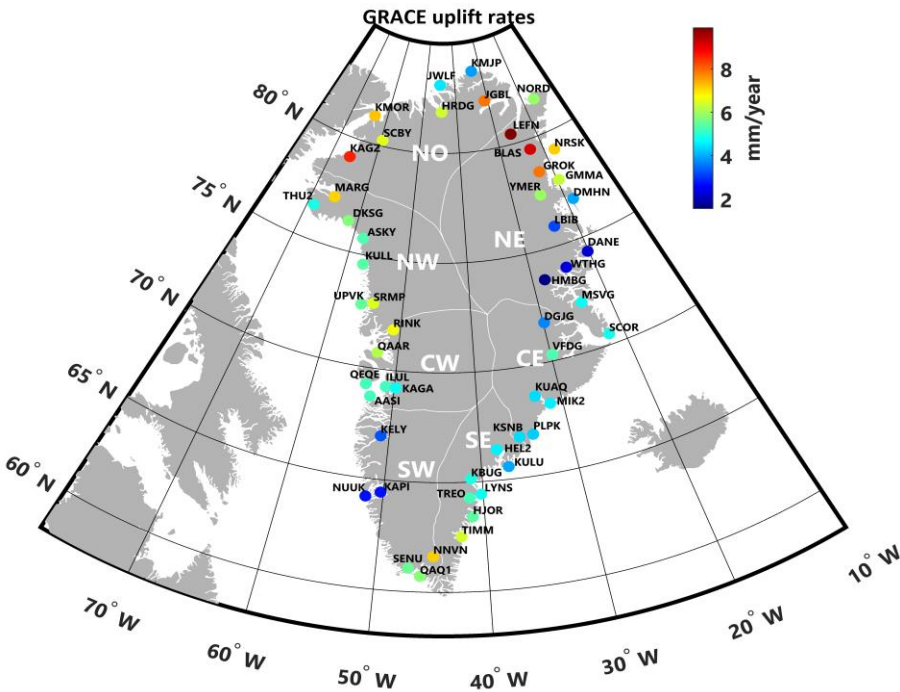
Elastic Up rate correction  
Khan et al. (2016)

GIA related land uplift rate = Up rate – Elastic correction

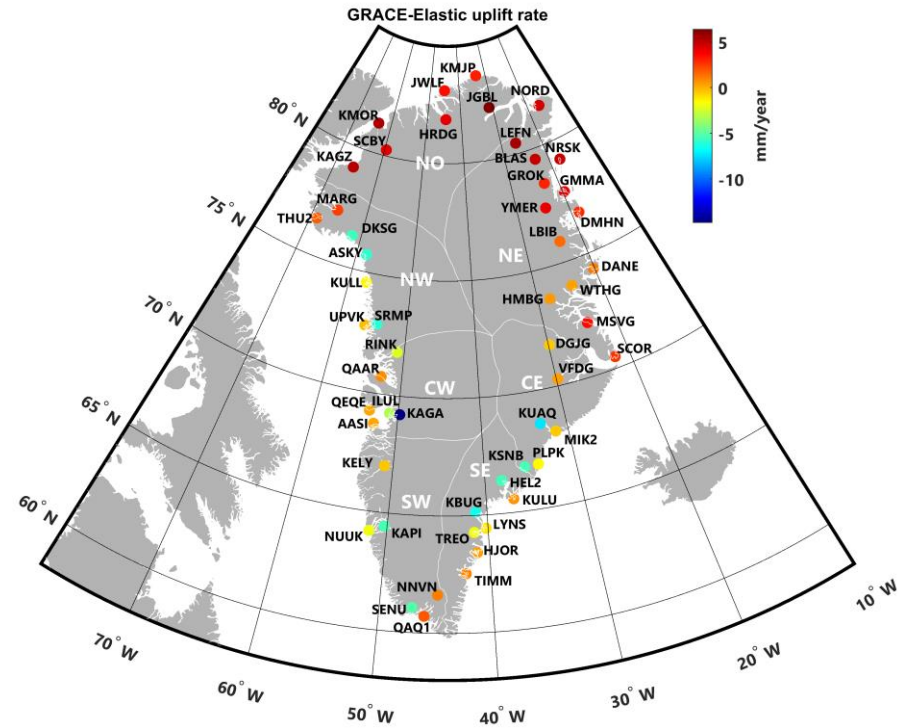
NASA's Airborne Topographic Mapper (ATM) 1995-2014  
ICESat from 2003-2009,  
Airborne Land, Vegetation, and Ice Sensor (LVIS) 2007-2013  
CryoSat-2 2010-2015,  
ERS-1 and ERS-2 data 1995-2003

Volume loss rate → mass loss rate (Kuipers Munneke et al., 2015)

# Land uplift rate model using GRACE data CSR RL05 2003-2015



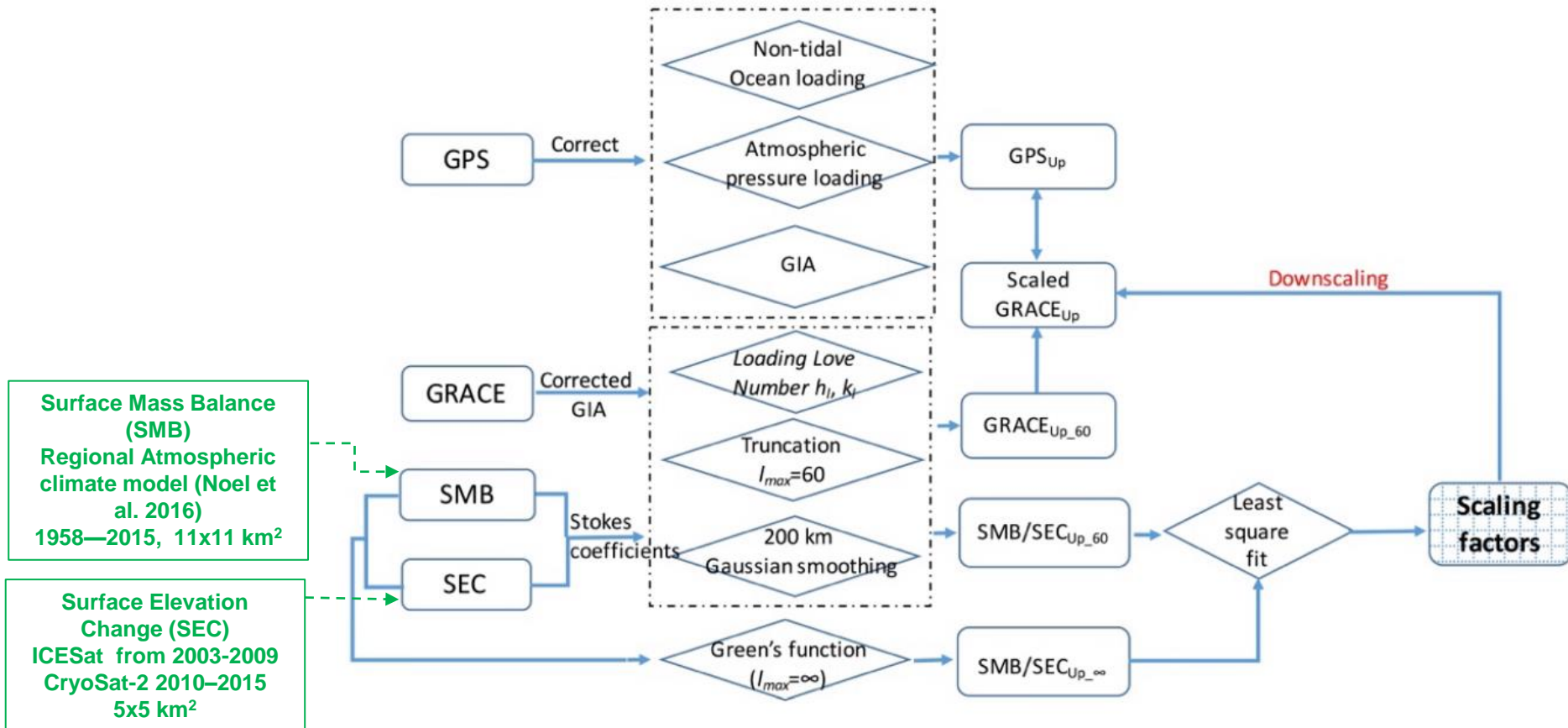
**BEFORE ELASTIC  
CORRECTION**



**AFTER ELASTIC  
CORRECTION**

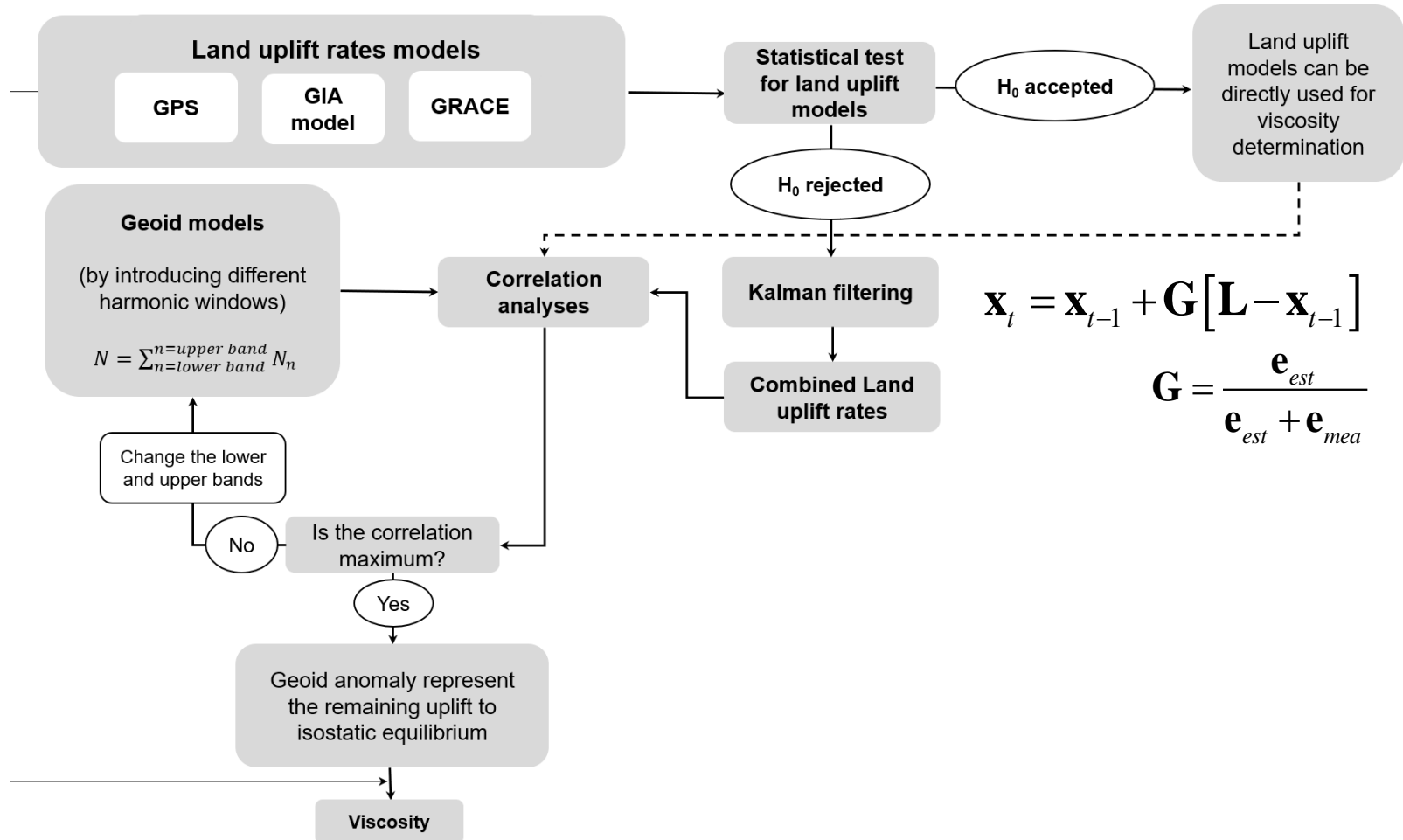


# Land uplift rate model using GRACE data (downscaling) according to Wang et al. (2019)



Wang et al. (2019)

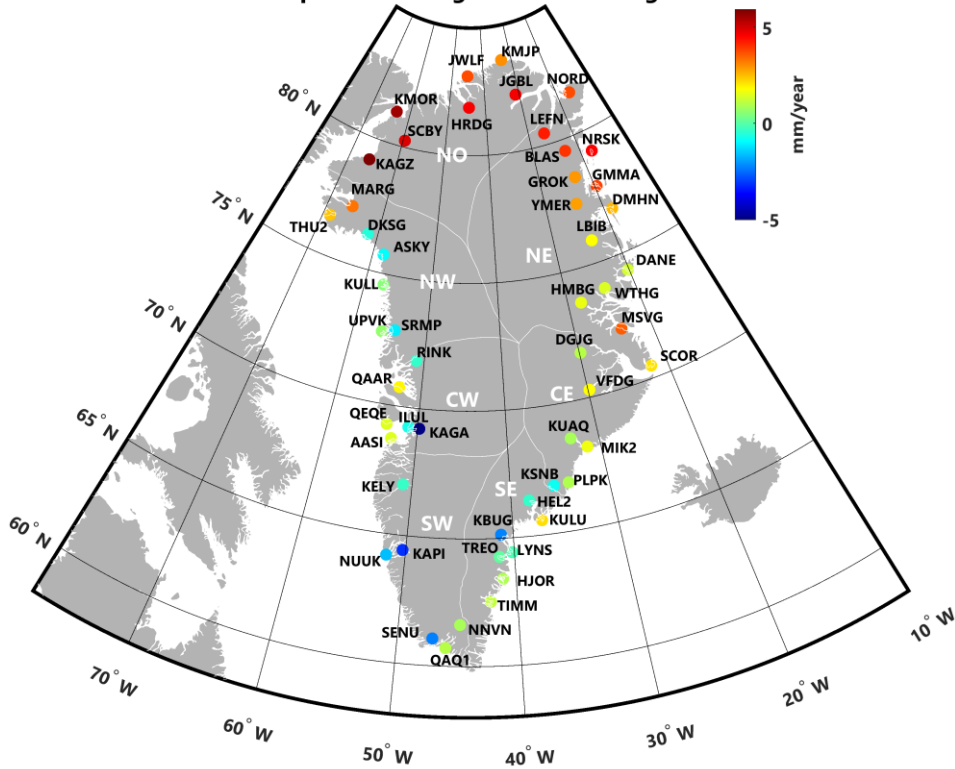
# Flowchart of viscosity determination using geoid anomaly and different land uplift rates



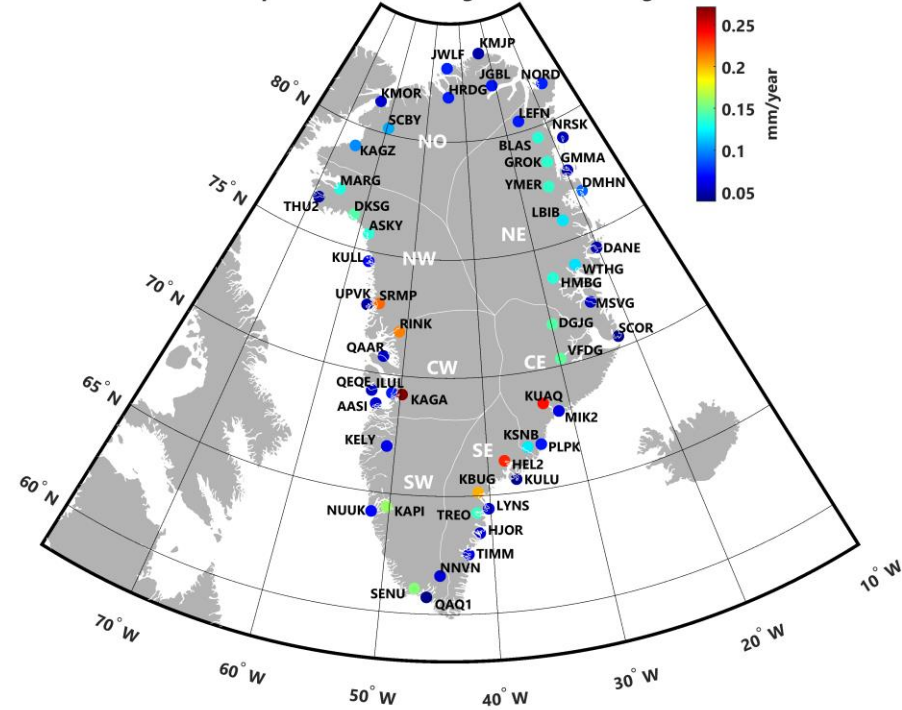


# Combined land uplift rate derived by Kalman filtering method (GPS + GRACE + GIA models)

Uplift rate using Kalman Filtering



Uplift rate error using Kalman Filtering

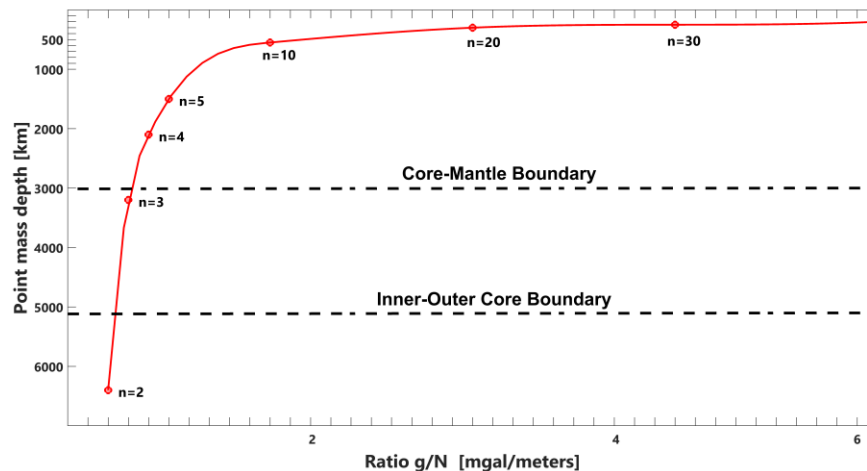


# Mantle viscosity using different land uplift and geoid models

$$\eta \approx -\frac{\gamma^2}{4\pi G} \sum_{n=0}^{\infty} \frac{2n+1}{2n+4+3/n} \frac{N_n}{\dot{h}_n}$$

Scenarios	Geoid model	Land uplift model	Harmonic window ( $N_n$ )	Correlation coefficient	Viscosity (Unit: Pa s)	Uncertainty (Unit: Pa s)
Scenario 1	EGM2008	ICE-6G (VM5a)	$10 \leq n \leq 39$	0.65	$1.9 \times 10^{22}$	-----
Scenario 2		Caron et al. 2018	$11 \leq n \leq 26$	0.68	$9.2 \times 10^{21}$	$1.2 \times 10^{17}$
Scenario 3		GNET	$18 \leq n \leq 25$	0.40	$1.3 \times 10^{21}$	$2.6 \times 10^{16}$
Scenario 4		GRACE	$11 \leq n \leq 26$	0.68	$5.1 \times 10^{21}$	$1.2 \times 10^{17}$
Scenario 5		Combined model	$11 \leq n \leq 26$	0.68	$7.8 \times 10^{21}$	$1.4 \times 10^{17}$

Ratio of gravity to geoid anomalies as a function of depth to a point-mass source. ed circles along the curve show corresponding harmonic degrees (The figure modified after Bowin, 2000).



# Comparison with the other studies

	Upper mantle viscosity (Pa s)	Lower mantle viscosity (Pa s)
This study	$9.2 \times 10^{21}$ Scenario 2 $5.1 \times 10^{21}$ Scenario 4 $7.8 \times 10^{21}$ Scenario 5	
Lambeck et al., 2017	$0.51 \times 10^{21}$	$13 \times 10^{21}$
Peltier et al., 2015	$0.5 \times 10^{21}$	$1.57 \times 10^{21}$
Roy & Peltier, 2017	$0.5 \times 10^{21}$	-----
Lau et al., 2016	$0.3 \times 10^{21}$	$1.0 \times 10^{21}$
Paulson et al., 2007	-----	$2.3 \times 10^{21}$
Caron et al., 2018	$0.6 \times 10^{21}$	$2.3 \times 10^{21}$
Zhao, 2013	$0.37 \times 10^{21}$	$1.9 \times 10^{21}$
Argus et al., 2021	$0.5 \times 10^{21}$	$1.6 \times 10^{21}$
Adhikari et al., 2021	$0.5 \times 10^{21}$	-----
<b>Average</b>	-----	$3.8 \times 10^{21}$

# Conclusion

- The evaluation shows that the uplift rates are different statistically; therefore, one will determine different viscosity values using individual land uplift models.
  - The Kalman filtering method was applied to estimate a combined land uplift model, which can compensate for the discrepancies.
- The obtained results in this study are comparable with the other studies performed by other scholars:
  - The obtained viscosities are between  $1.3 \times 10^{21}$  and  $1.9 \times 10^{22}$  Pa
  - Depending on different radial boundaries in the mantle varying from 250 to 700 km.
  - The results are over half order of magnitude greater than the estimates in the literature. Although the results are also close to Paulson et al., (2007) and Caron et al., (2018) i.e.  $2.3 \times 10^{21}$  Pa s for the lower mantle viscosity.
  - The reason can be the low correlation of GIA-related gravity field and land uplift rate and the uncertainty of input data
    - Elastic correction
    - GRACE data
    - GIA models
    - GPS data
- The proposed method is more straightforward and consequently faster.

**Thank you for your attention!**